AD-A093 173 DAVID W TAYLOR NAVAL SHIP RESEARCH AND DEVELOPMENT CE--ETC F/G 11/8
PERFORMANCE CHARACTERISTICS OF OIL LUBRICATED SWING-PAD THRUST --ETC(
DEC 80 N T SIDES, T L DAUGHERTY

UNCLASSIFIED DTNSRDC-80/122 NL

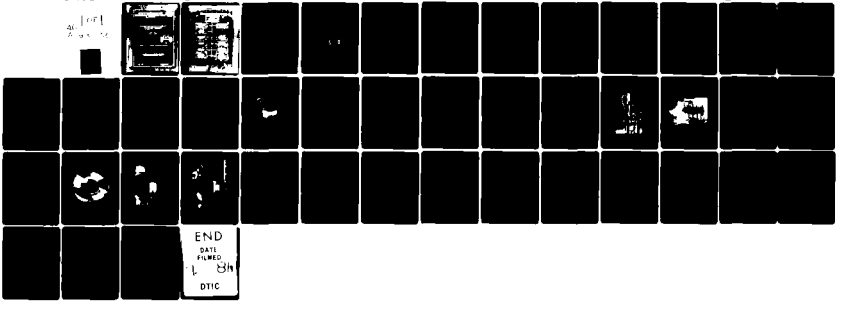

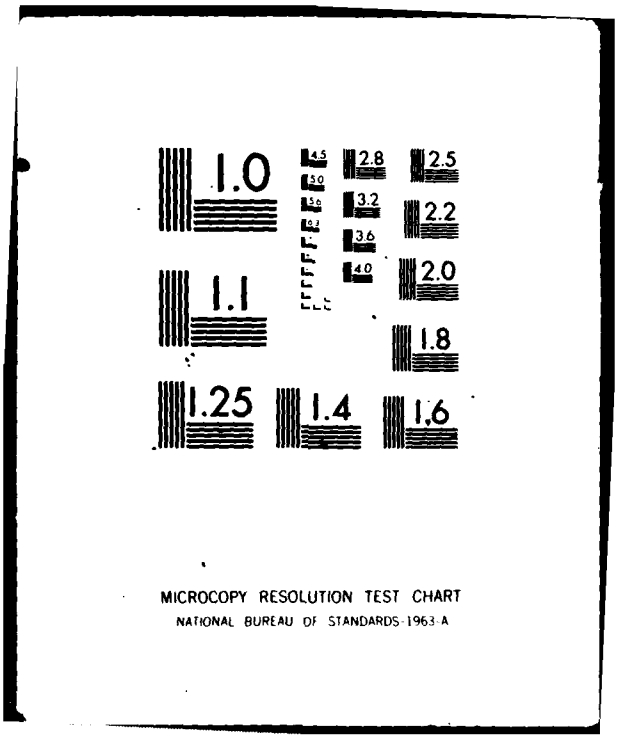
1.0
1.1
1.25
1.4
1.6
1.8
2.0
2.2
2.5
2.8
3.2
3.6
4.0
4.5
5.0
MICROCOPY RESOLUTION TEST CHART
NATIONAL BUREAU OF STANDARDS-1963-A

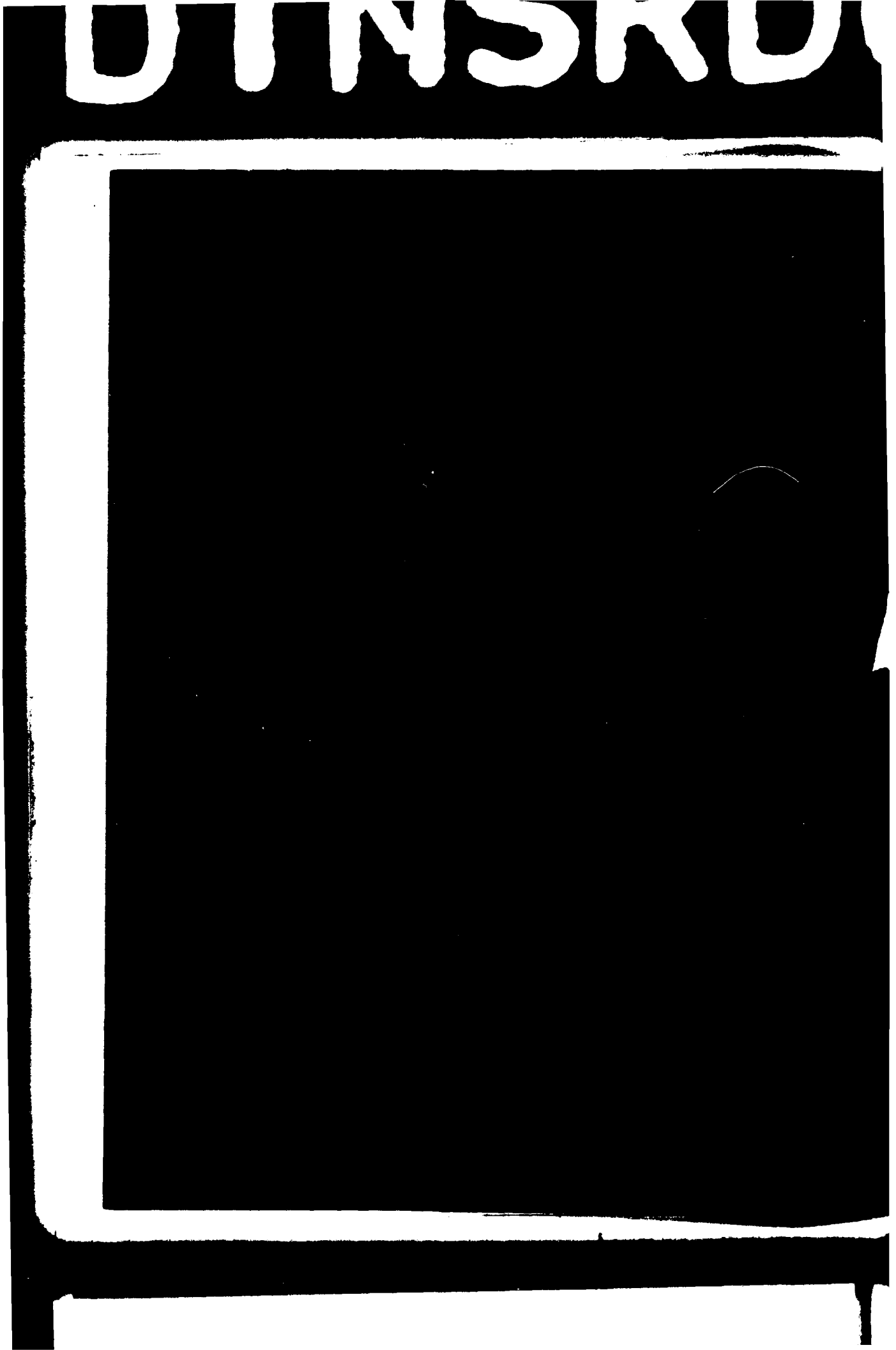

UNCLASSIFIED

SECURITY CLASSIFICATION OF THIS PAGE (When Data Entered)

REPORT DOCUMENTATION PAGE

READ INSTRUCTIONS BEFORE COMPLETING FORM

1. REPORT NUMBER: DTNSRDC-80/122	2. GOVT ACCESSION NO.: AD-A093 273
3. RECIPIENT'S CATALOG NUMBER	
4. TITLE (and Subtitle): PERFORMANCE CHARACTERISTICS OF OIL LUBRICATED SWING-PAD THRUST BEARINGS WITH DIFFERENT RADII OF CURVATURES.	5. TYPE OF REPORT & PERIOD COVERED: Final Repts.
	6. PERFORMING ORG. REPORT NUMBER
7. AUTHOR(s): Nathan T. Sides, Thomas L. Daugherty (16) F66522	8. CONTRACT OR GRANT NUMBER(s)
9. PERFORMING ORGANIZATION NAME AND ADDRESS: David W. Taylor Naval Ship R&D Center, Bethesda, Maryland 20084	10. PROGRAM ELEMENT, PROJECT, TASK AREA & WORK UNIT NUMBERS: See reverse side.
11. CONTROLLING OFFICE NAME AND ADDRESS: (17) ZF66522001	12. REPORT DATE: December 1980 (11)
	13. NUMBER OF PAGES: 40 (12) 45
14. MONITORING AGENCY NAME & ADDRESS(if different from Controlling Office)	15. SECURITY CLASS. (of this report): UNCLASSIFIED
	15a. DECLASSIFICATION/DOWNGRADING SCHEDULE

16. DISTRIBUTION STATEMENT (of this Report)

APPROVED FOR PUBLIC RELEASE; DISTRIBUTION UNLIMITED.

17. DISTRIBUTION STATEMENT (of the abstract entered in Block 20, if different from Report)

18. SUPPLEMENTARY NOTES

19. KEY WORDS (Continue on reverse side if necessary and identify by block number)

Bearing
Thrust Bearing
Friction
Hydrodynamic Lubrication

20. ABSTRACT (Continue on reverse side if necessary and identify by block number)

Frictional performance of oil lubricated thrust bearings of conventional tilt-pad and swing-pad designs is presented. Results from the conventional tilt-pad bearing are used as a baseline. All tests were conducted at a speed of 35 rpm and a sump temperature of 50 C (122 F). Thrust load was increased in increments generally from 2,069 kPa (300 psi) until onset of mixed lubrication. All bearings were tested with the pad surfaces in the centered and

(Continued on reverse side)

DD FORM 1 JAN 73 1473 EDITION OF 1 NOV 65 IS OBSOLETE S/N 0102-LF-014-6601

UNCLASSIFIED

SECURITY CLASSIFICATION OF THIS PAGE (When Data Entered)

BLOCK 10

Program Element 62766N
Task Area ZF 66-512-001
Work Unit 2832-122

BLOCK 20 (continued)

off-centered positions. Various radii of curvature were evaluated in the swing-pad version. Friction results for all bearings in the hydrodynamic region compared favorably with conventional hydrodynamic theory. The hydrodynamic load capacity of one version of the swing-pad design was 79 percent greater than that of the centered tilt-pad bearing. Improvements in performance were observed in the regions of hydrodynamic and mixed lubrication by offsetting the pad surfaces for the tilt-pad and elastomeric swing-pad bearings. Performance for the elastomeric swing-pad bearing improved as a function of decreased radius of curvature in the laminates.

TABLE OF CONTENTS

LIST OF FIGURES

LIST OF TABLES

NOTATION

a	(h_i/h_o)
B	Bearing pad circumferential length, cm (in.)
b	Bearing pad radial length, cm (in.)
d	Moment arm from P_r to pad centerline, cm (in.)
F	Friction force, N (lb)
f	Coefficient of friction
F_f	Force due to friction, N (lb)
h_i	Lubricant film thickness at leading edge, mm (in.)
h_o	Lubricant minimum film thickness at trailing edge, mm (in.)
K_f	Function of η
K_p	Function of η
M_f	Moment due to friction force, N-m (lb-in.)
M_p	Moment due to pressure forces, N-m (lb-in.)
P	Average load on bearing surface, kPa (psi)
P_r	Resultant pressure vector, N (lb)
R	Radius of swing, cm (in.)
U	Surface speed, m/s (in./s)
W	Total bearing applied load, N (lb)
x	Distance from pad leading edge to pivot point, cm (in.)
η	Modifying factor
μ	Absolute viscosity, poise (reyns)

ABSTRACT

Frictional performance of oil lubricated thrust bearings of conventional tilt-pad and swing-pad designs is presented. Results from the conventional tilt-pad bearing are used as a baseline. All tests were conducted at a speed of 35 rpm and a sump temperature of 50 C (122 F). Thrust load was increased in increments generally from 2,069 kPa (300 psi) until onset of mixed lubrication. All bearings were tested with the pad surfaces in the centered and off-centered positions. Various radii of curvature were evaluated in the swing-pad version. Friction results for all bearings in the hydrodynamic region compared favorably with conventional hydrodynamic theory. The hydrodynamic load capacity of one version of the swing-pad design was 79 percent greater than that of the centered tilt-pad bearing. Improvements in performance were observed in the regions of hydrodynamic and mixed lubrication by offsetting the pad surfaces for the tilt-pad and elastomeric swing-pad bearings. Performance for the elastomeric swing-pad bearing improved as a function of decrease in the laminates.

ADMINISTRATIVE INFORMATION

This report covers work conducted under an in-house Independent Exploratory Development Program under Program Element 62766N, Task Area ZF66-512-001, and Work Unit 2832-122.

INTRODUCTION

The swing-pad bearing is designed to encourage formation of a hydrodynamic wedge by swing-like motion of its surface. This swing-like motion is encouraged by the deflections under normal pressure loading and surface friction forces. Below the bearing surface a series of metal and elastomer laminations deflect in an arcuate manner to form a desirable lubricant film between the bearing surface and the moving surface. The layers of metal and elastomer must have a radius of curvature which is less than that of the radius to the surface of the pad.
The swing-pad bearing was invented at the Center.* Its characteristics were demonstrated[1]** in a series of exploratory thrust and journal bearing experiments.

---

*Patent number 3,930,691 of 6 January 1976.

**A complete list of references is given on page 35.

Comparison of the frictional characteristics and load capacity were made[2] between two variations of the swing-pad and a conventional tilt-pad thrust bearing. The present investigation consists of a comparison of swing-pad thrust bearings with different radii of curvature in the laminations.

APPROACH

Friction in hydrodynamic sliding surface bearings is a function of the viscosity of the lubricant, surface speed of the bearing, applied load, and the size of the bearing pad. The friction of thrust bearings of tilt-pad and swing-pad designs was measured on the same test machine at a fixed speed of 35 rpm and a sump temperature of 50 C (122 F). Bearing load was increased in increments generally from 2,069 kPa (300 psi) until onset of mixed lubrication. The tilt-pad bearing, purchased commercially, was used as a reference. Two swing-pad bearing designs were evaluated. All bearings were tested with the center of tilt or swing centered and offset to one side. Comparison of frictional results was also made with that predicted by existing theroretical analysis.[3,4,5] The load capacity in the hydrodynamic region and the mixed lubrication region of each design were compared. Results obtained from previous work[2] are included in this report to permit an overall comparison.

THEORETICAL BASIS

Theoretical analysis of hydrodynamic bearings is based upon the existence of a converging wedge such as that shown in Figure 1. Hydrodynamic theory applied to a tapered wedge gives the following equations, according to Fuller[3]

$$h_o = \left(\frac{6 \mu U B \eta K_p}{P} \right)^{1/2} \tag{1}$$

$$F = \mu b \; B \; K_f \frac{U}{h_o} \tag{2}$$

$$f = \frac{F}{W} \tag{3}$$

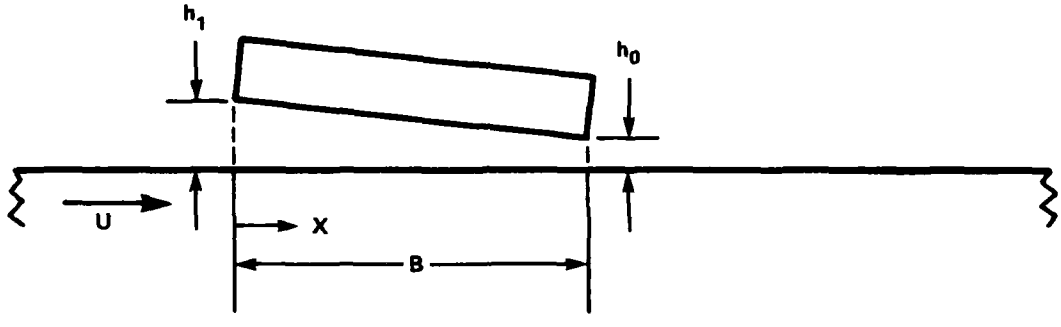

Figure 1 - Hydrodynamic Converging Tapered Wedge

For the purposes of this investigation, the following values apply (see Figure 2):

$$B = 3.18 \text{ cm } (1.25 \text{ in.})$$

$$b = 2.97 \text{ cm } (1.17 \text{ in.})$$

$$\frac{b}{B} \approx 1, \text{ therefore, } \eta = 0.44$$

Assuming the leading edge film thickness to be twice the trailing edge film thickness, then $a = 2$, $K_p = 0.0265$, and $K_f = 0.773$. From Equation (3),

$$f = \frac{F}{PbB} \tag{4}$$

combining Equations (1), (2), and (4) gives

$$f = \frac{\mu b B K_f U}{\left(\frac{6\mu UB\eta K_p}{P}\right)^{1/2}} \cdot \frac{1}{PbB} \tag{5}$$

Simplifying and applying numerical values,

$$f = 2.9 \left(\frac{\mu U}{PB}\right)^{1/2} \tag{6}$$

When plotted on log-log graph paper, the above expression yields a straight line. Simplifying Equation (1), the following expression is obtained for the minimum film thickness.

$$h_o = 0.264 \left(\frac{\mu UB}{P}\right)^{1/2} \tag{7}$$

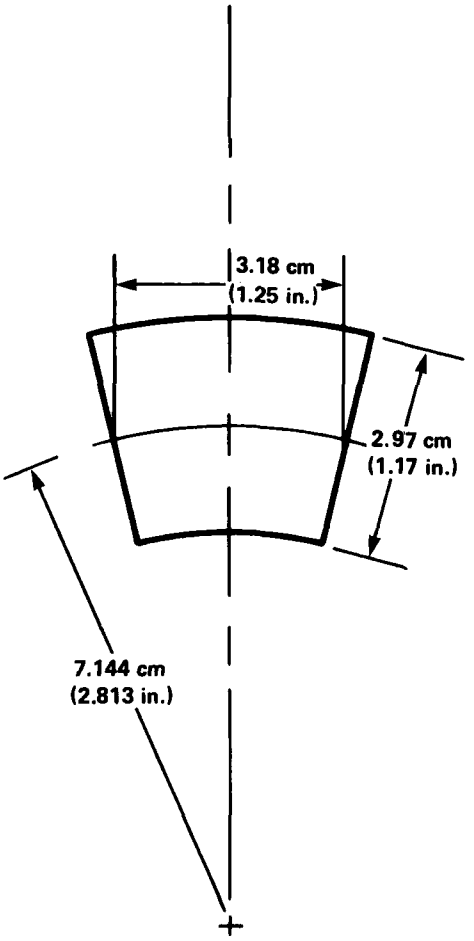

Figure 2 - Shoe Dimensions

Hydrodynamic lubrication is said to exist as long as the bearing behaves according to the above expressions. Full fluid separation exists between the bearing and the mating runner surface and the only frictional losses are due to fluid shear. Under these conditions, virtually no wear occurs and bearing life is theoretically infinite. The coefficient of friction decreases in proportion to the parameter, $(\mu U/PB)^{1/2}$. Load is supported entirely by the pressurized lubricant.

In practice, however, a limit to hydrodynamic lubrication exists. As the parameter $\mu U/PB$ is decreased through increased load, decreased speed, or viscosity of the lubricant, the minimum film thickness of the lubricant is also reduced. A point is reached when the height of the asperities on the bearing and runner surfaces exceeds the thickness of the fluid film and intermittent contact occurs. The coefficient of friction will continue to decrease to a minimum value. The slope will depart from the straight line observed in the hydrodynamic region. Continued decreases in $\mu U/PB$ will produce a sudden increase in the coefficient of friction. This transitional region of operation, characterized by the load being shared by both asperity contacts and pressurized lubricant, is commonly referred to as mixed lubrication.

Further reduction in $\mu U/PB$ leads to further deterioration to the point that load is completely supported by surface-to-surface contact where the lubricant no longer separates the bearing and runner. The coefficient of friction then will be large and will reflect the frictional properties of the mating materials. This condition is known as boundary lubrication.

TILT-PAD BEARING

The conventional tilt-pad thrust bearing consists of individual pads usually ranging in number from two to twelve and spaced annularly as shown in Figure 3. It consists of a flat sliding surface, or runner, sliding over the pads which are free to pivot or tilt independently. The pads are usually completely immersed in the lubricant. The tilt-pad (or pivoted pad) thrust bearing was invented independently by A. Kingsbury and A.G.M. Michell in the early 1900's. The basic theory behind this design is that the pivoted shoe is free to adjust itself to the optimum angle for any operating condition. Its basic load capacity is derived by creation of a converging wedge of lubricant in the direction of motion. Behavior is similar to

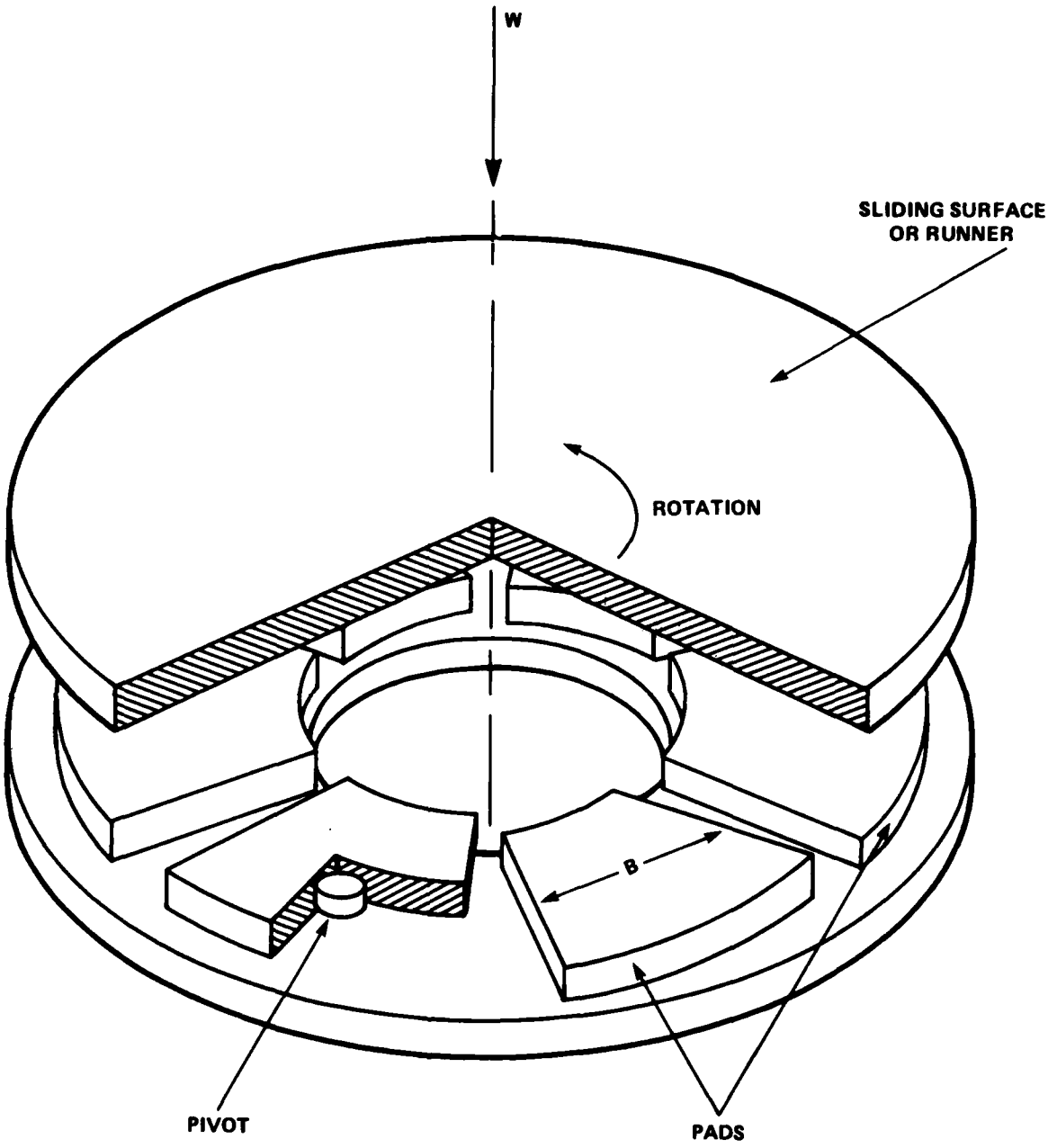

Figure 3 - Typical Tilt-Pad Thrust Bearing Assembly

that discussed in the theoretical basis section of this report. The pivot location may be moved to various positions across the width of the pad. The center of pressure must be located at the pivot position to achieve equilibrium[6] (see Figure 4). A centrally pivoted bearing allows operation in both directions of rotation. From a theoretical standpoint, however, a flat surfaced centrally pivoted bearing with constant lubricant viscosity has zero load-carrying capacity.[7] In practice, it has been found that centrally pivoted pads have significant load-carrying capacity. The explanation[7,8,9] for this paradox is that load-carrying capacity is produced by two primary effects. First, the viscosity gradient of the lubricant across the pad surface generates a finite load-carrying capacity. The viscosity changes as a result of work done upon the lubricant as it passes across the bearing. Secondly, the shape of the pad surfaces creates a change in the pressure profile and influences the load capacity. Convex surfaces with a certain amount of curvature offer important advantages. These may be produced in several ways. Some degree of crowning usually results from the manufacturing process used in finishing the pads. The leading and trailing edges of the pad are normally chamfered during manufacture. Elastic deformations under load result from the single point support of the pressure distribution on the pad surface. Deformations due to thermal gradients in the pad itself may also contribute to this crowning.

Assuming rigid flat pad surfaces and constant lubricant viscosity, an expression has been derived[8] for the location of the center of pressure in terms of the amount of offset. The optimum pivot location is found to correspond to an offset of 0.58 of the length of the bearing, toward the trailing edge.

SWING-PAD BEARING

The swing-pad thrust bearing is designed to be a hydrodynamic bearing, and as such is expected to have operating characteristics similar to those described earlier. Like the tilt-pad thrust bearing, it consists of a series of individual pads, as shown in Figure 3. One version of the swing-pad thrust bearing is shown in Figure 5 and consists of a set of three spherical metal shims separated by elastomer laminates. These components are assembled between a mounting base and a surface platform. In contrast to the tilt-pad design, the swing-pad bearing is designed with its center of pivot or "swing" located above the bearing face instead of behind it; see Figure 6. The primary objective of the laminates is to provide

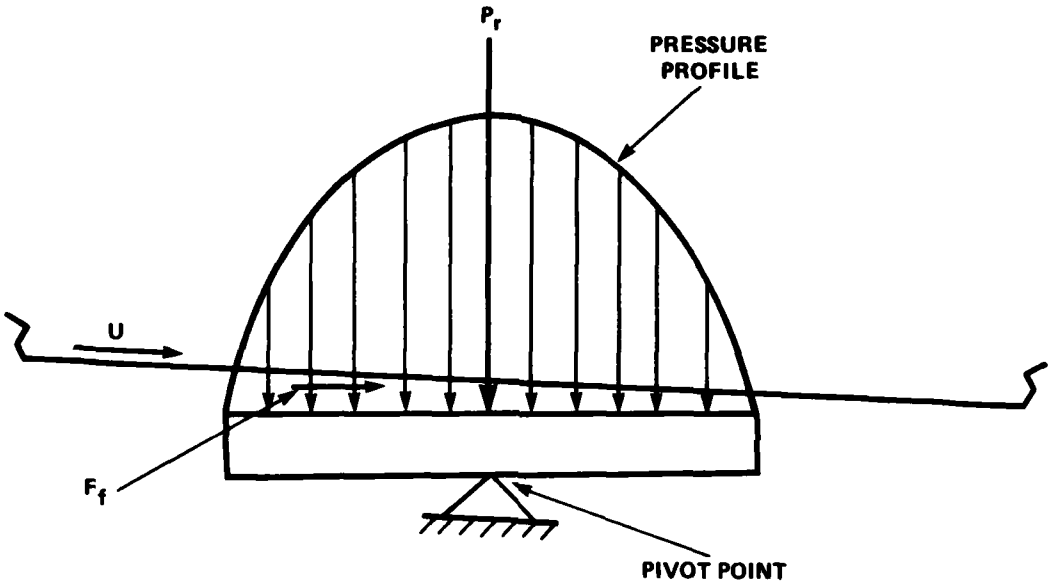

Figure 4 - Pressure Distribution on Tilt-Pad Bearing

1 CENTER OF SWING
2 SWING RADIUS
3 BABBITT SURFACE
4 SURFACE PLATFORM
5 ELASTOMER LAMINATES
6 MOUNTING BASE
7 METAL SHIMS

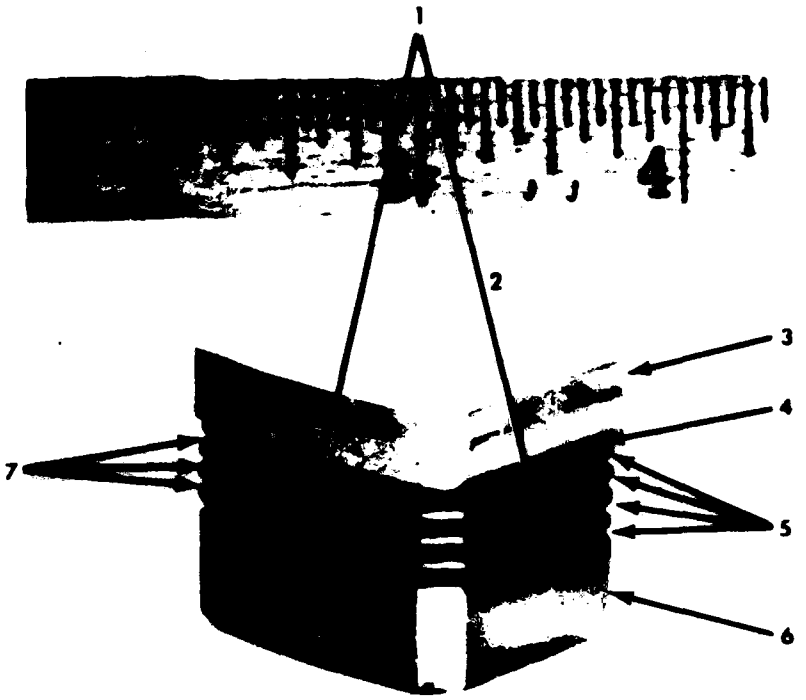

Figure 5 - Swing-Pad Bearing, Centered

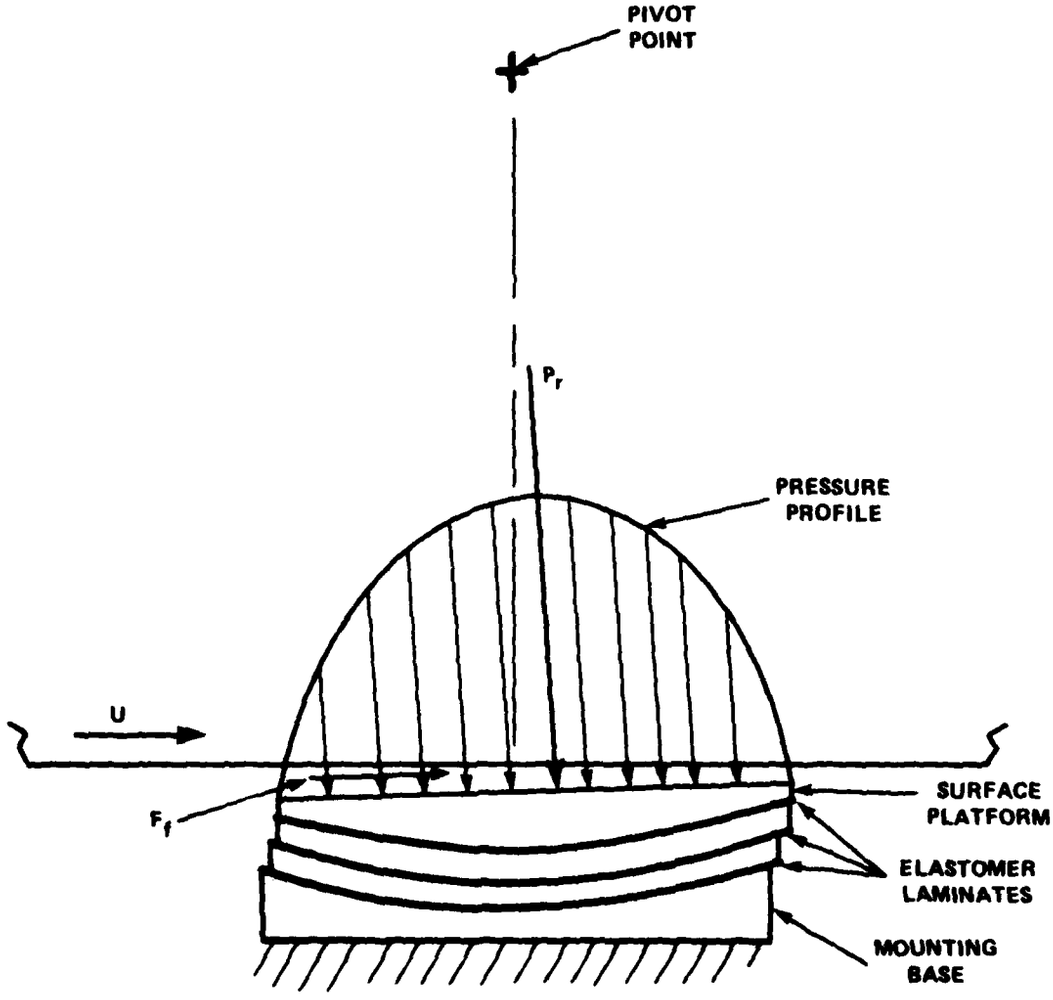

Figure 6 - Pressure Distribution of Swing-Pad Bearing

high compressive and low shear stiffness. High compressive stiffness is desirable in practical applications to control and maintain shaft position. Low shear stiffness allows the bearing surface to displace along its swing arc to the desired converging wedge. An idealized version of the swing-pad bearing can be approximated by minimizing the shear stiffness while providing very high compressive stiffness. This design is referred to as the hybrid-pad bearing. It consists of replacing the elastomer and metal spherical laminates with steel balls which ride between hardened spherical surfaces; see Figure 7.

Note that the center of pressure on the pad surface is not required to pass through the center of swing as was required in the tilt-pad bearing analysis. For example, if the pad surface were offset toward the leading edge (see Figure 8), a significant moment is created by this offset which encourages a converging wedge.

The conventional theory of hydrodynamic sliding surface bearings considers only the pressure loading and location of the center of pressure on the surface of the pads. Drag or friction forces are usually ignored. This is a quite acceptable procedure when operation is clearly in the hydrodynamic region. However, as operation moves into the transition between hydrodynamic and mixed lubrication it becomes apparent that the frictional forces play a more significant role. For the tilt-pad bearing with its center of pivot located behind the pad surface a friction force on the surface produces a moment in a direction opposing desirable converging wedge formation; see Figure 4. For the swing-pad design with its center of swing located above the pad surface, the friction force on the surface produces a moment in the direction of desirable converging wedge formation; see Figure 6. Operation in the hydrodynamic region with the same wedge angle should provide the same performance for both the tilt-pad or swing-pad designs. The range of hydrodynamic lubrication and mixed lubrication would be expected to be extended with proper swing-pad design due to the location of the swing center.

The radius of curvature of the laminates is expected to play an important role in determining the wedge formation under a given pressure and friction force. For a given normal force acting at a fixed distance from the centerline of the bearing, the wedge angle increases as the radius of curvature gets smaller. The same effect results from a shear force applied parallel to the bearing surface.

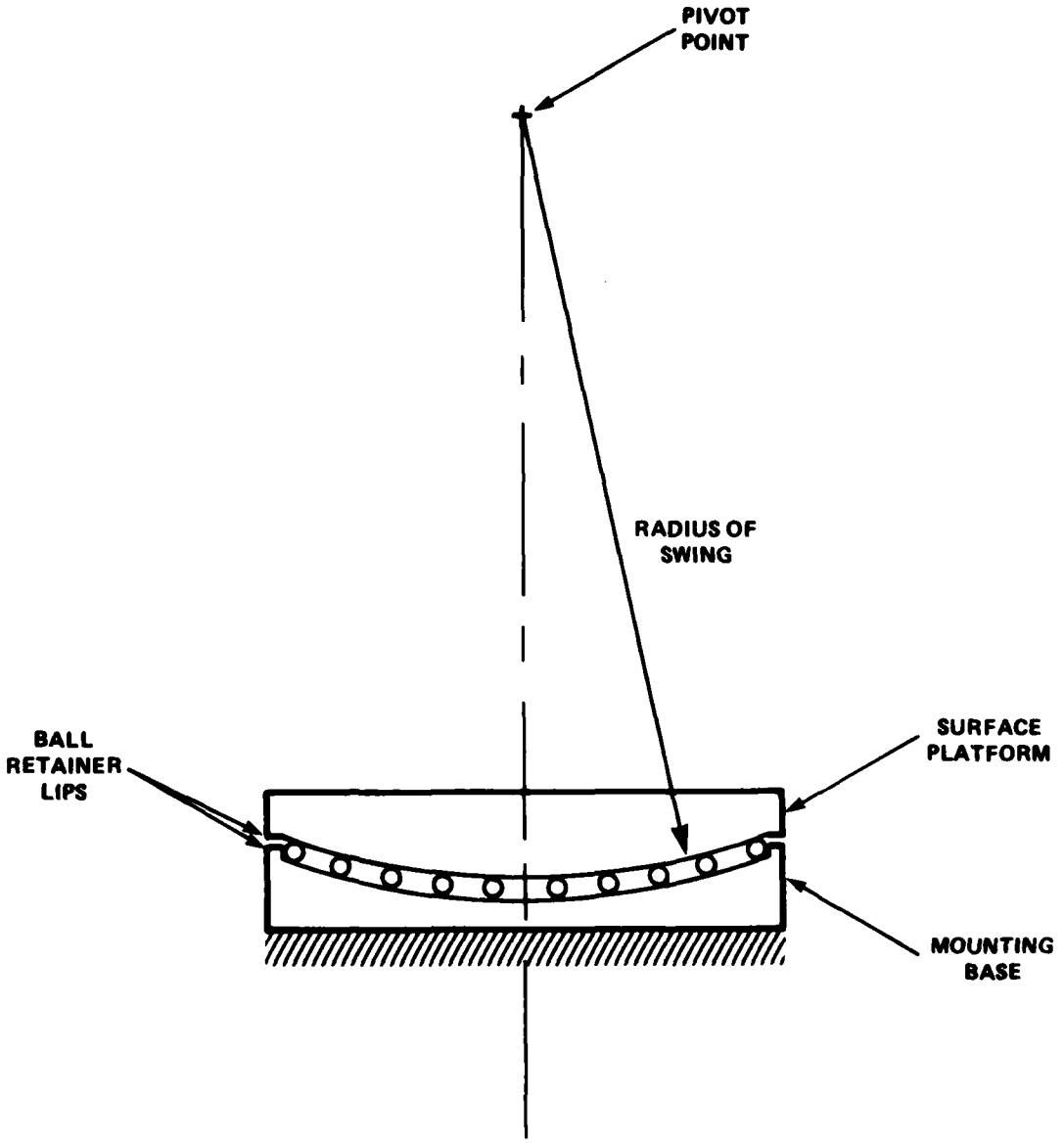

Figure 7 - Hybrid-Pad Bearing

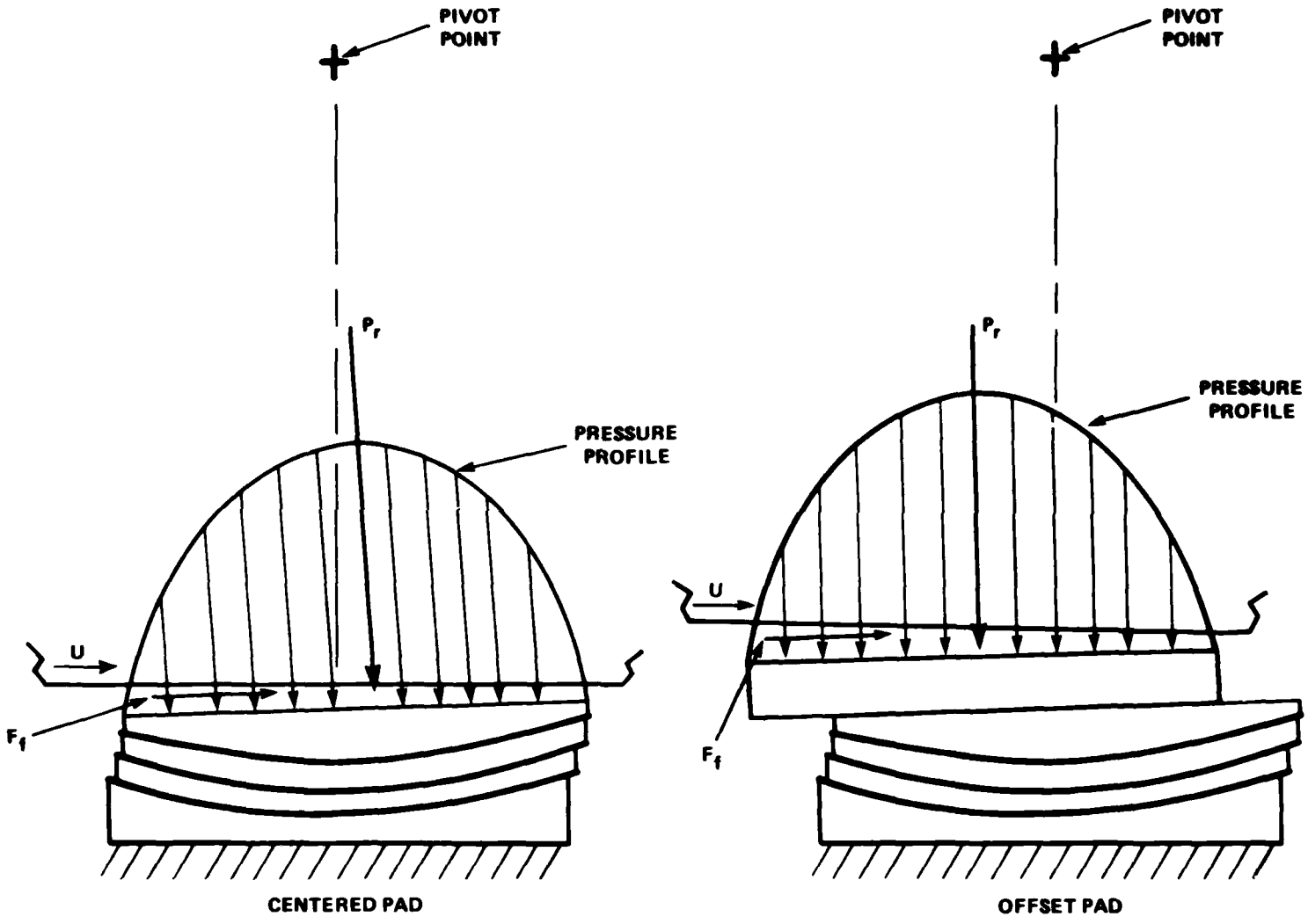

Figure 8 - Centered and Offset Swing-Pad Bearing

EQUIPMENT, MATERIALS, AND PROCEDURES

The test machine (see Figures 9, 10, and 11) uses a hydraulic drive system coupled to a gearbox capable of bi-directional rotation. Two disk runners are splined on the shaft and are free to move axially in the vertical direction. Two sets of bearing pads, each consisting of three pads located 120 degrees apart, are loaded against the disk runners. The arrangement is very similar to an automobile disk brake system. Loading is accomplished with hydraulic cylinders. The bearing pads and runner assembly is submerged in a lubricant reservoir. The reservoir is made of plexiglas to allow viewing. A heat exchanger is also incorporated to regulate the bulk lubricant temperature.

Measured parameters are shaft speed, torque via an inline torquemeter, load via load cells and pressure gauges, and bulk lubricant temperature via a thermcouple.

The runner surfaces used in all tests were mild steel ground and polished circumferentially to a surface finish of 0.10-0.20 μm (4-8 μin.) rms as measured in the direction of rotation. Bearing shoes were made of babbitt of the following composition:

Tin	89.60 percent
Lead	0.14 percent
Antimony	7.99 percent
Copper	2.16 percent

This composition is very similar to ASTM babbitt grade 2 and Navy grade 2.

The babbitt shoes of 0.64 cm (0.25 in.) thickness were cemented to the bearing pads. Two steel pins were used also to carry the shear load and maintain the relative position of the shoe to the pad. Two sets of three pads each were mounted on loading rings. The shoes were then manually polished by placing the assembly against a rotating polishing disk. Emery paper of successively finer grades (down to 600 grit) was used on the polishing disk and kept constantly wet to prevent clogging. Rotation of the polishing wheel was always in the same direction as that of the runner disk in the test machine. Surface finishes of 0.10-0.15 μm (4-6 μin.) rms were achieved on the babbitt surfaces in this manner.

The two bearing sets were mounted in the test machine and the shaft rotated at 35 rpm with no load. The temperature of the lubricant was regulated at 50 C (122 F). The lubricant used was 2190 TEP oil (MIL-L-17331) with a viscosity roughly equivalent to an SAE 20 oil. Thrust load was applied at approximately 2,069 kPa (300 psi) for 15 minutes and the following data were recorded: sump temperature, applied load,

1 HYDRAULIC MOTOR
2 REDUCTION GEAR
3 TORQUE SENSOR
4 OIL TANK
5 LOAD PISTON BLOCKS
6 HEATER

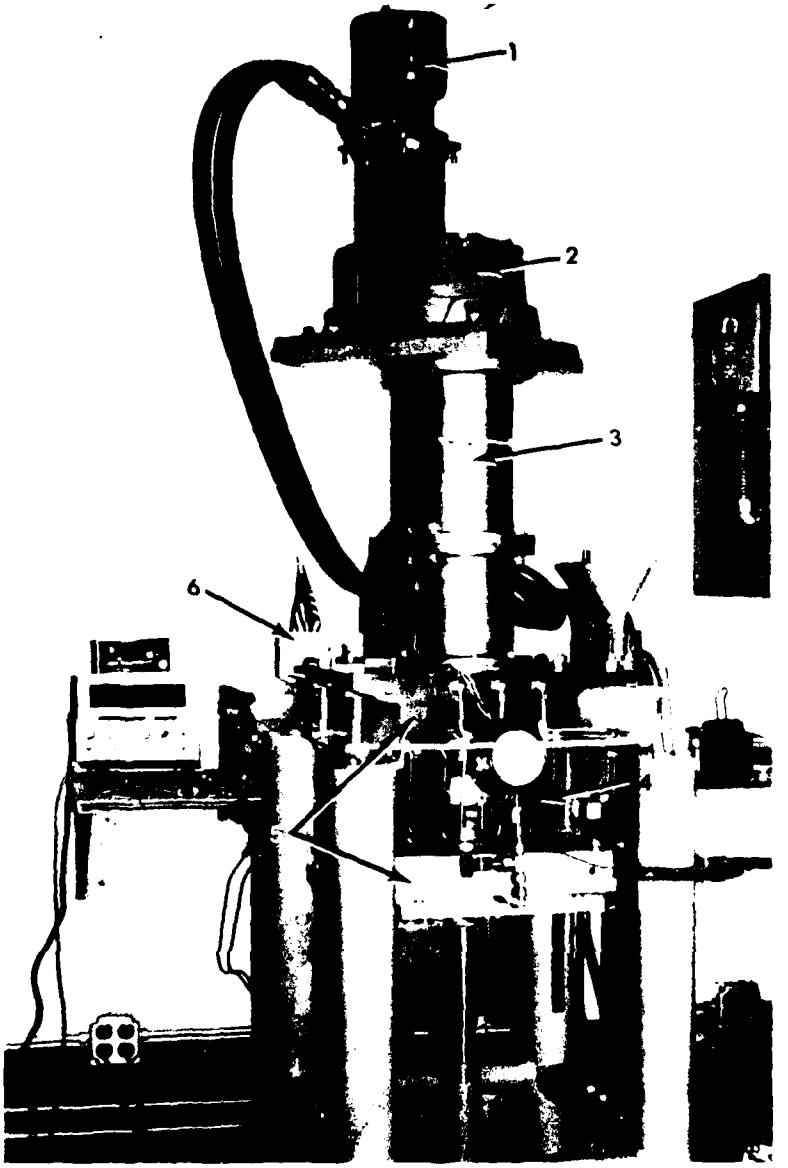

Figure 9 - Test Machine

1 HEATING COIL
2 RUNNER PLATES
3 TEST BEARING
4 THERMOCOUPLE

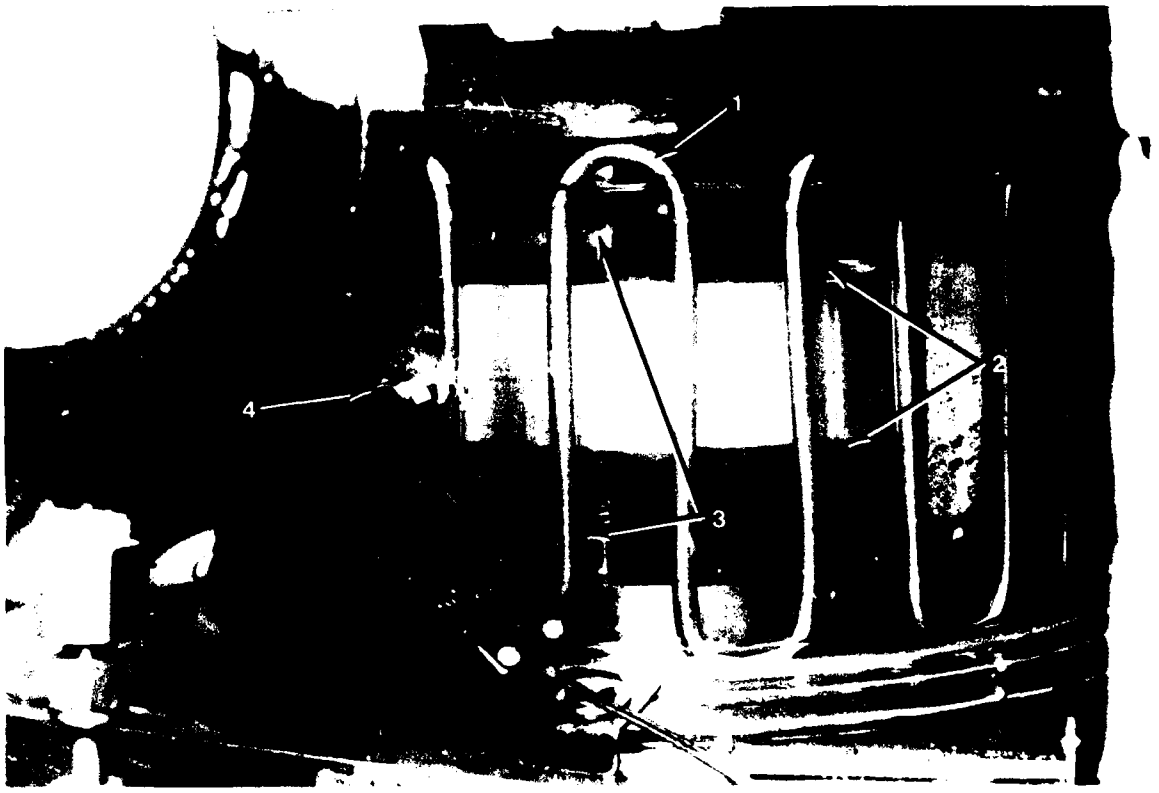

Figure 10 - Test Bearing in Oil Tank

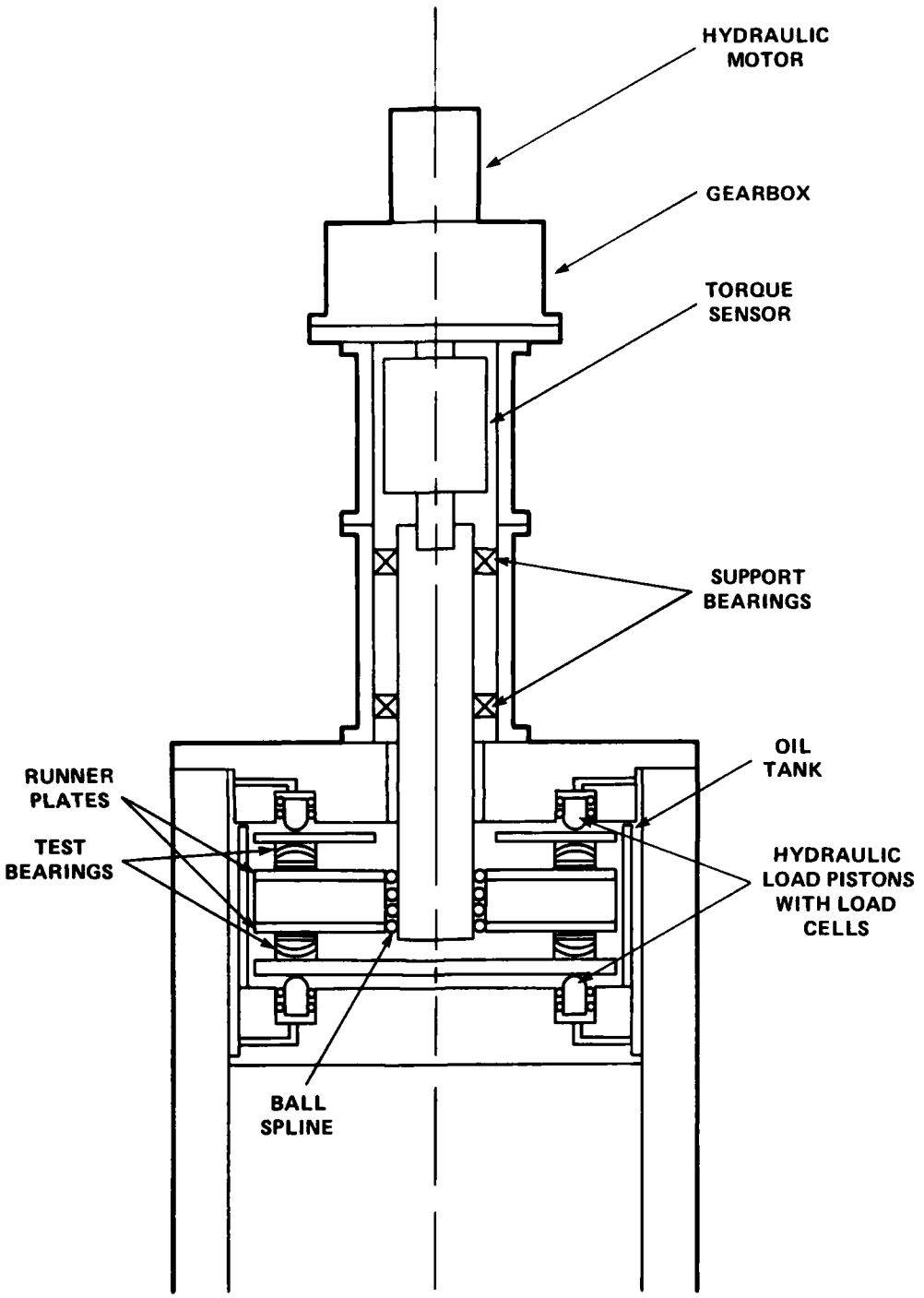

Figure 11 - Test Machine Schematic

shaft speed, and shaft torque. Applied load was increased in increments of approximately 1379 kPa (200 psi) through 13,792 kPa (2000 psi) and 2758 kPa (400 psi) beyond 13,792 kPa (2000 psi). Data were recorded after 15 minutes of operation at each condition. The coefficient of friction was computed and was found to decrease in value with increased load as long as the bearing remained in the hydrodynamic mode. When the coefficient of friction started increasing in value with increased load, signifying breakdown of the hydrodynamic film and entry into the mixed lubrication region, the test was stopped. The bearings were removed for inspection and photographs were taken.

An offset ratio of $x/B = 0.7$ was tested. Some preliminary testing with the swing-pad bearing showed that an offset of $x/B = 0.7$ produced the best results. The hybrid-pad bearing was expected to have similar performance to the swing-pad bearing and as such, $x/B = 0.7$ was adopted for it also. The coefficient of friction and the power losses for the tilt-pad bearing are relatively constant[5] for x/B values ranging from 0.57 to 0.75. The minimum film thickness is reduced[5] by 17 percent from its optimum value at $x/B = 0.7$. Therefore, $x/B = 0.7$ was used on this bearing as well for uniformity.

The tilt-pad and hybrid-pad bearings were both additionally tested at $x/B = 0.6$ in order to establish experimentally if any change in performance was detectable. The results are discussed later.

BEARINGS TESTED

The swing-pad bearing was fabricated at the Center. The manufacturing technique was developed and perfected with the assistance of the Center's rubber laboratory. The metallic components were fabricated in the machine shop. The laminates consisted of calendered sheets of Buna-N rubber that were vulcanized to the metal parts using a specially designed mold. The hardness of the cured rubber is 55±5 on the Shore A scale. Bearings with four different radii of curvature were fabricated; three were 2.54, 5.08, and 10.16 cm (1.00, 2.00, and 4.00 in.). The fourth had flat laminates representing an infinitely large radius. All bearings had four laminates. The pads were mounted 120 deg apart on a 7.144 cm (2.813 in.) radius-to-center of pad with a total surface area for the three pads of 26.5 cm^2 (4.1 $in.^2$). The tilt-pad bearing was purchased from Kingsbury Machine Works, Inc. It is a three shoe, self-alining, equalizing type with a radius of 6.668 cm (2.625 in.) to the pivot point. The surface area of the three pads is 79.4 cm^2 (12.3 $in.^2$). The tilt-pad

was first tested as received with the larger pad surface. Babbitt shoes identical to those used in the swing-pad were then bonded to the larger tilt-pad shoe (see Figure 12) and the tests conducted as described. Frictional results of both arrangements were compared to data obtained in a shipboard application. These results agreed well in all cases. It was concluded that no experimental error was being introduced by bonding smaller pad surfaces to the tilt-pad bearing assembly. The swing-pad and hybrid-pad bearing assemblies are shown in Figures 13 and 14, respectively. The spherical mating surfaces of the hybrid design were hardened to a value of 60 on the Rockwell C scale. The overall dimensions and the "swing" radius were identical to those of the swing-pad.

RESULTS

The results are presented in Figures 15 through 18 and Tables 1 through 4. Figure 15 presents typical friction data of the dynamic tests for each bearing design. The coefficient of friction calculated from the torque measurements was plotted against the parameter, $\mu U/PB$. A theoretical curve is also shown representing hydrodynamic conditions according to Equation (6). The friction curve has three distinct regions. The first is the region where the experimental data are parallel to the predicted hydrodynamic behavior. The second region is characterized by departure from parallelism with the hydrodynamic curve but undergoing minor changes in friction with increased bearing load. The third region is represented by abrupt changes in friction coefficient with increased load. The curve is marked with the following symbols: o, representing the last condition indicative of hydrodynamic behavior; and □, representing the last transition point before the onset of a sudden increase in the coefficient of friction as load is increased. Data under these conditions are used as a basis of comparison for each of the bearing designs and are used in Tables 1 through 4. The load at the point marked with symbol o is referred to in this report as the "hydrodynamic load capacity" because it represents the highest load obtained under hydrodynamic conditions. Figure 18 is a bar graph representation of the results in Tables 1 through 4. Figures 16 and 17 present the performances of the swing-pad and hybrid-pad as a function of the radius of curvature.

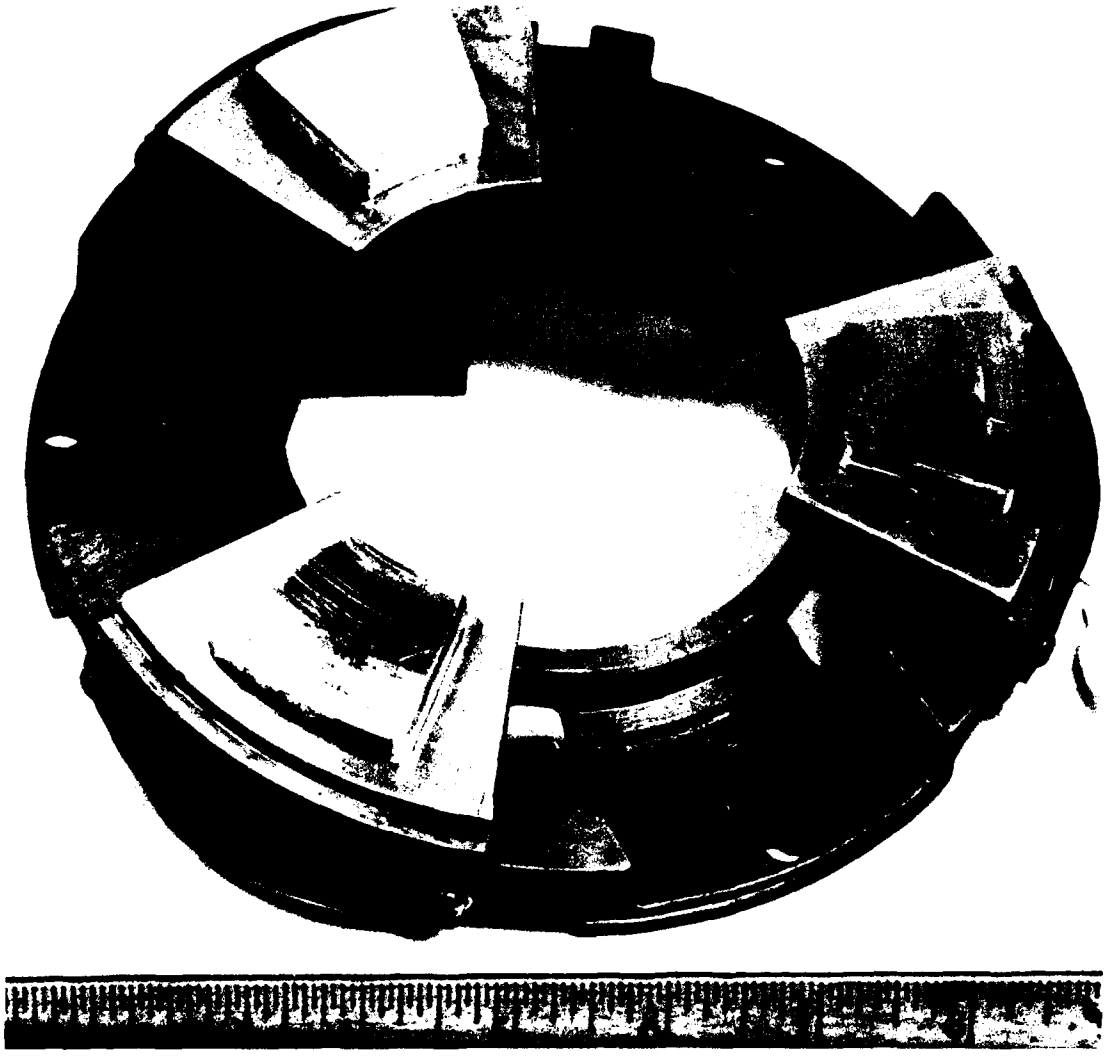

Figure 12 - Tilt-Pad Assembly, Centered (After Test)

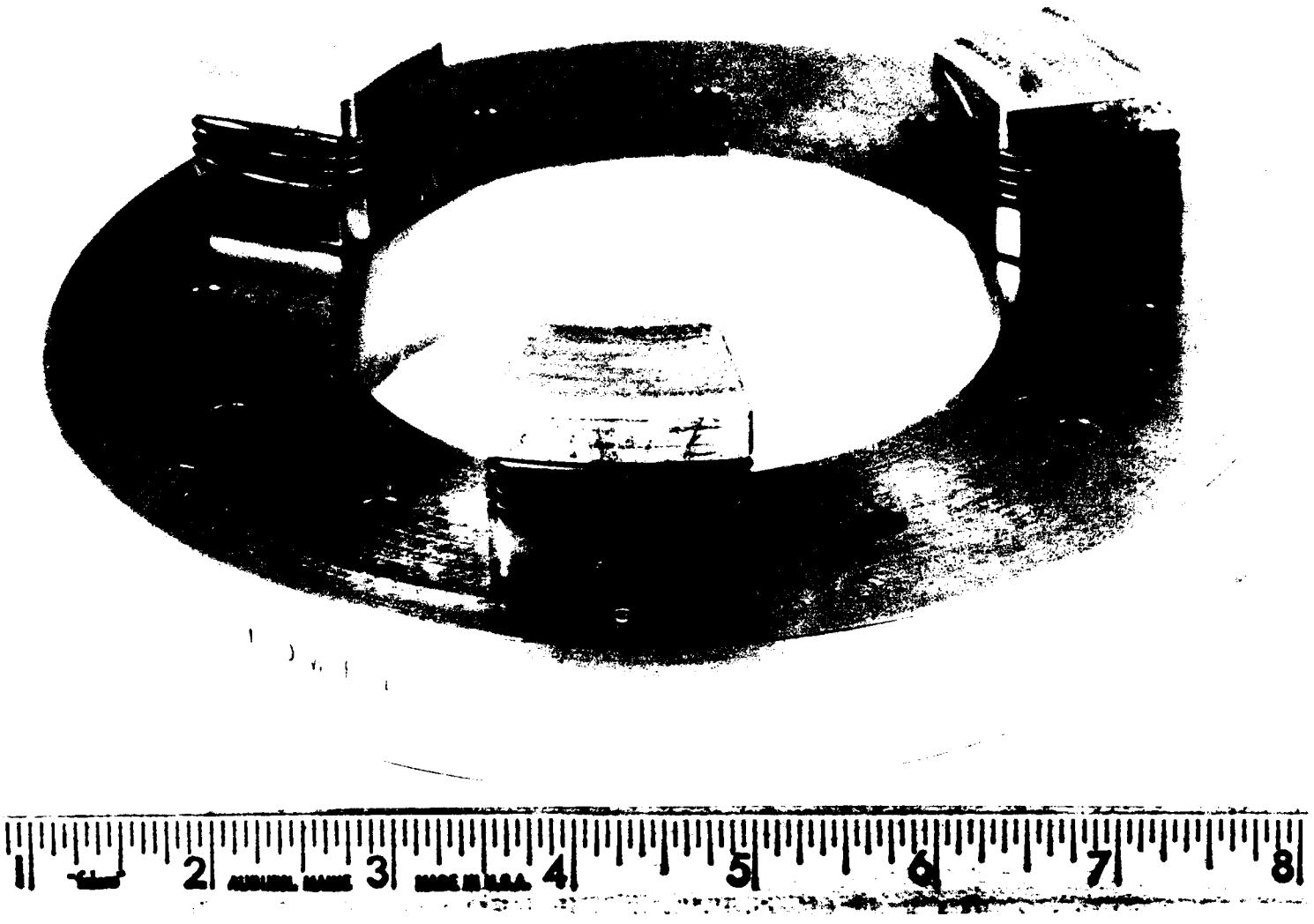

Figure 13 - Swing-Pad Assembly, Centered

Figure 14 - Hybrid-Pad Assembly, Centered

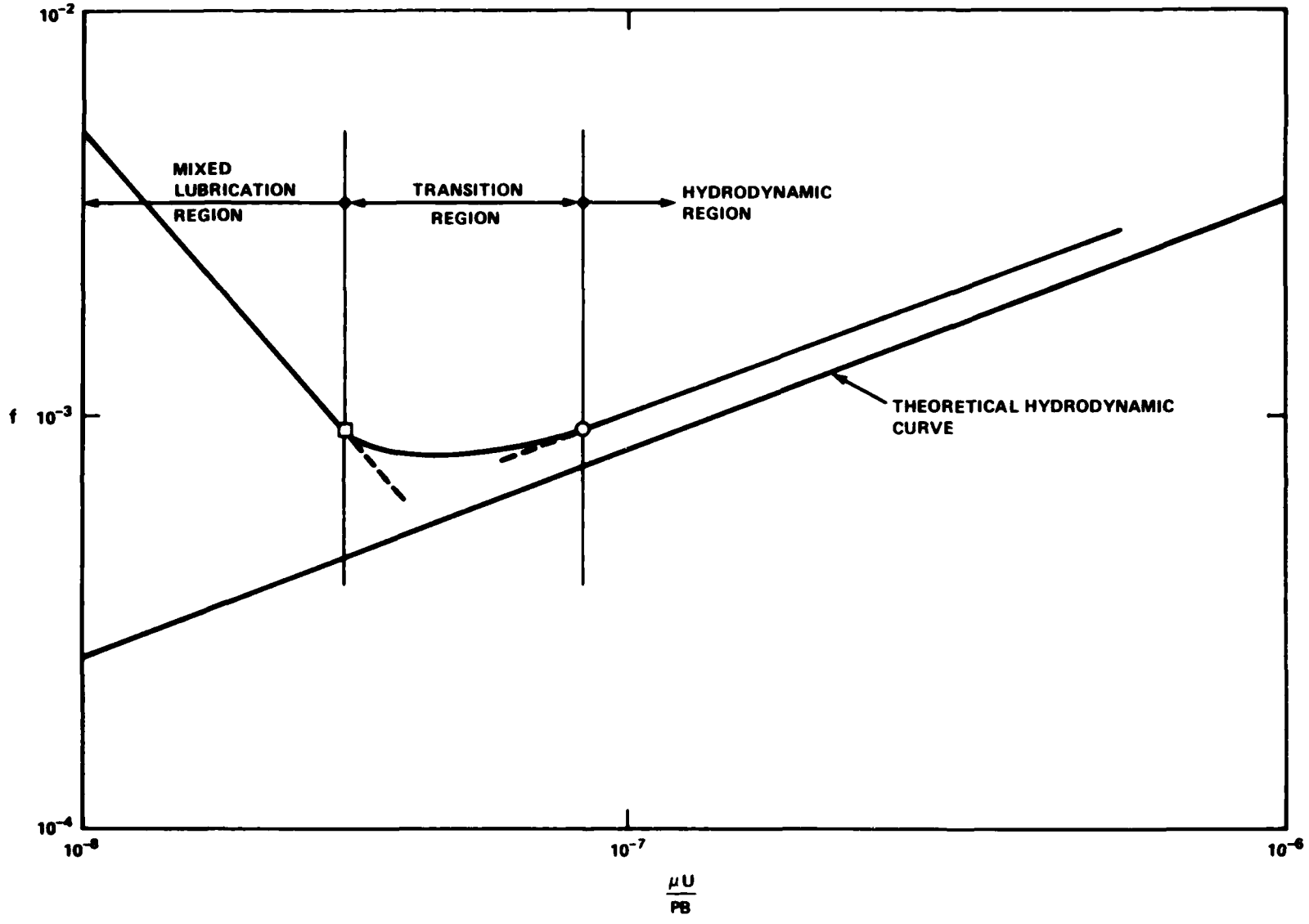

Figure 15 - Typical Friction Curve

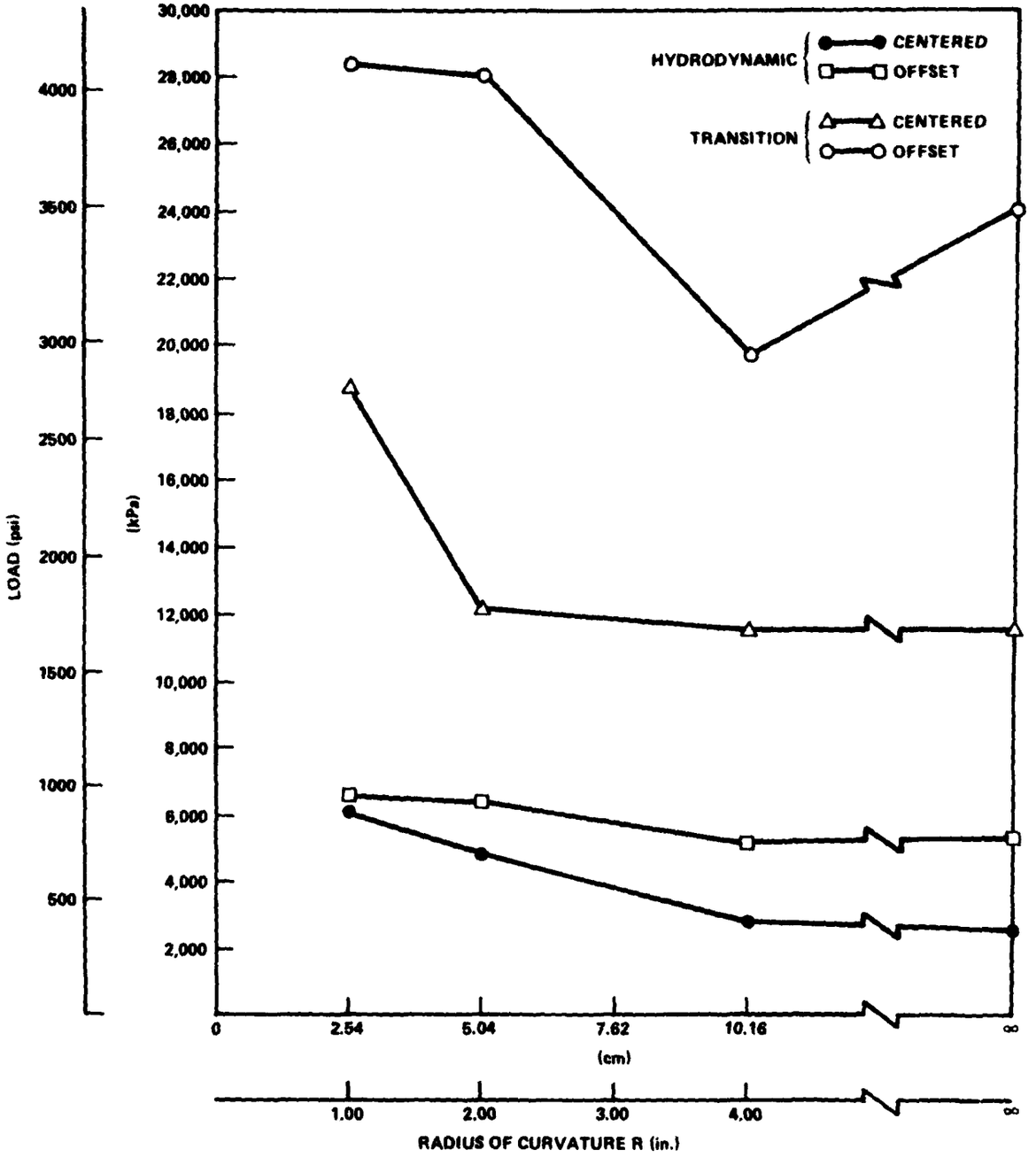

Figure 16 - Swing-Pad Bearing as a Function of Radius of Curvature

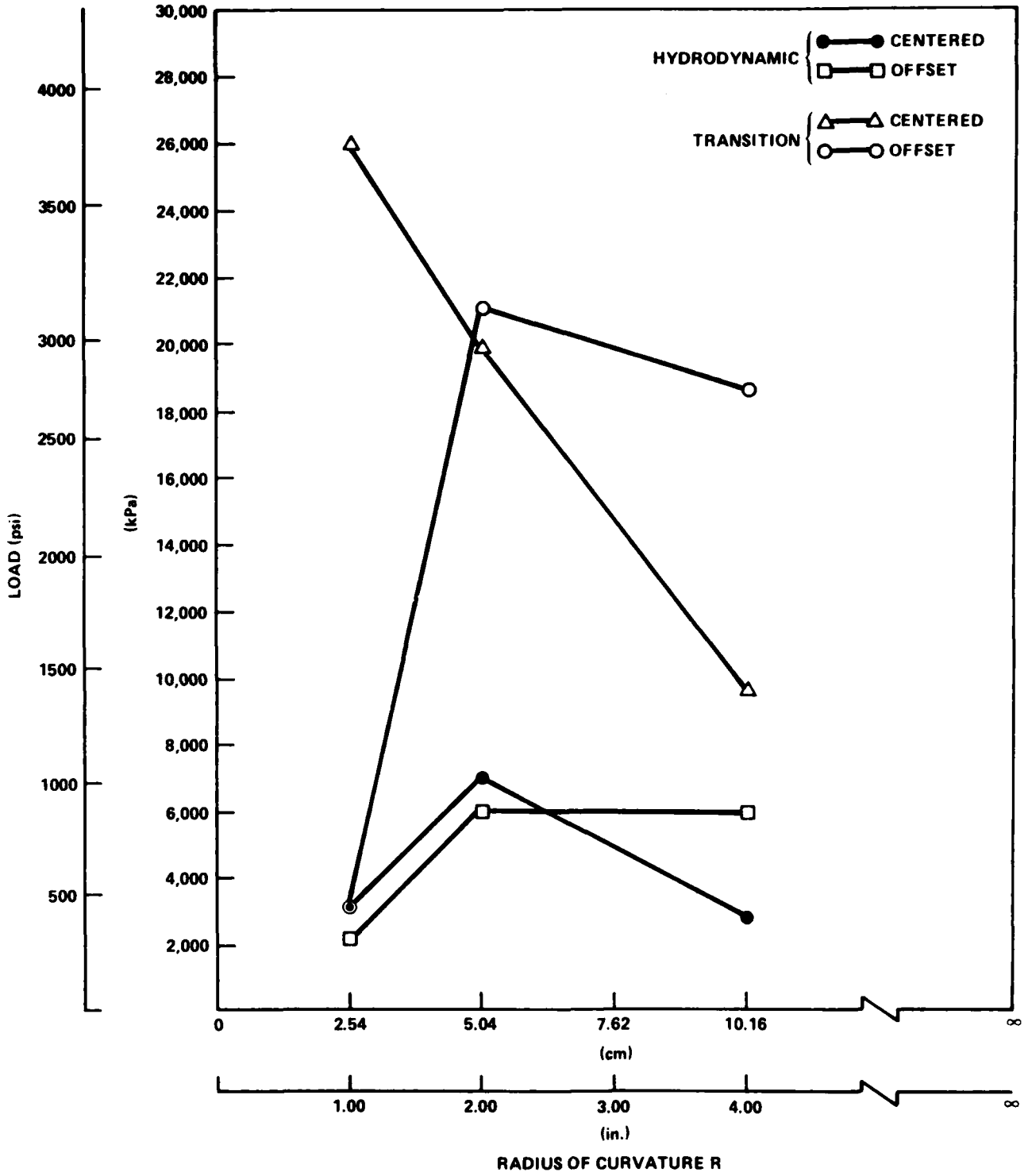

Figure 17 - Hybrid-Pad Bearing as a Function of Radius of Curvature

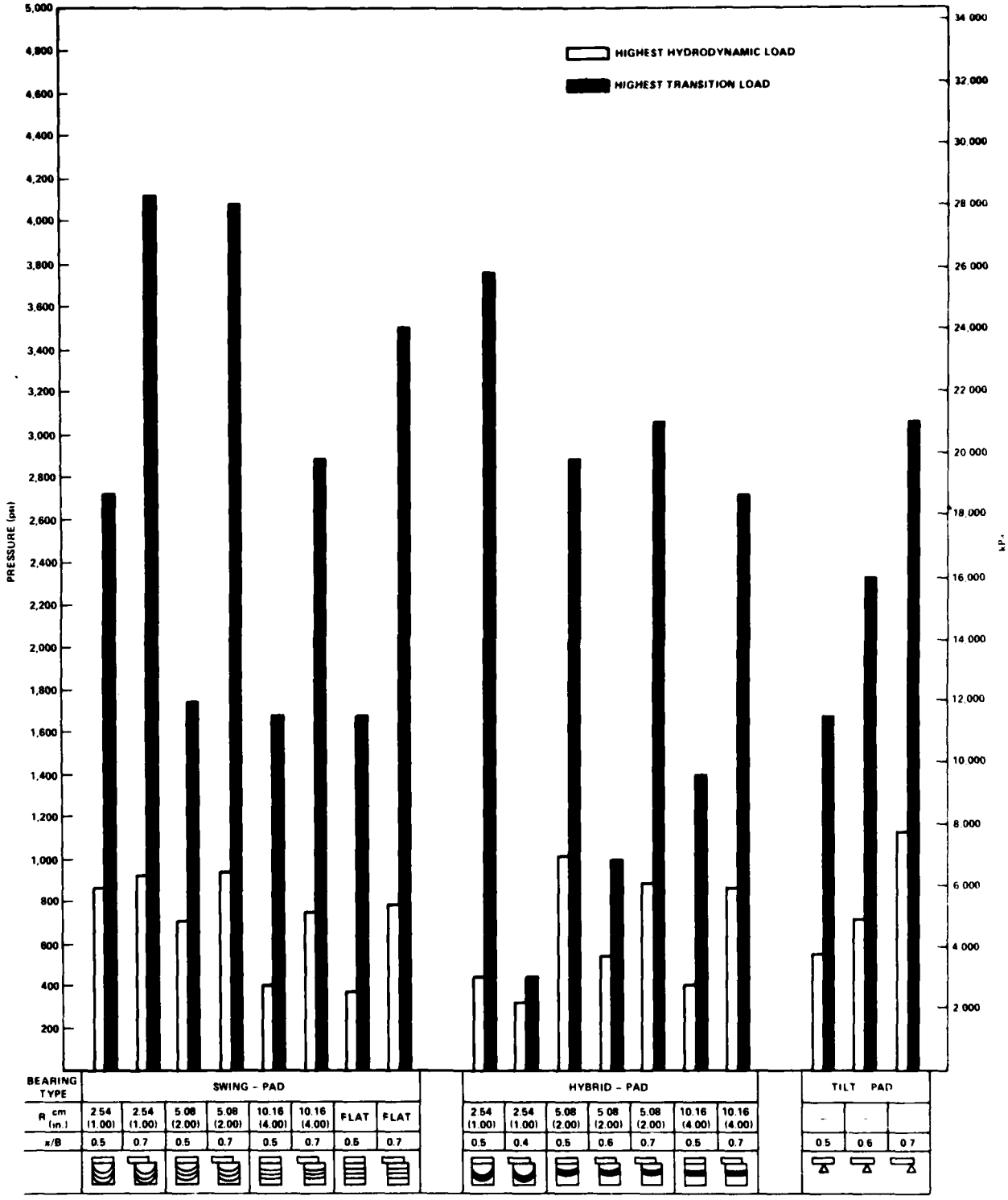

Figure 18 - Comparison of Load Capacity

DISCUSSION

Frictional results, as typified in Figure 15, showed that all bearings exhibited behavior characteristics of hydrodynamic conditions for higher values of $\mu U/PB$. For each bearing design, the magnitude of the friction coefficient was higher than that predicted by theory. This is expected because the measured torque contains not only the shear losses predicted by theory in the lubricant film but also drag of the rotating parts in the oil reservoir and the turbulence between the pads. The friction predicted is also dependent upon the ratio of inlet film thickness to minimum film thickness. The intent of the theoretical friction curve is to provide a reference to determine the type of lubrication existing under various test conditions.

Tables 1 through 4 list the coefficient of friction and value of $\mu U/PB$ for the last point indicative of hydrodynamic conditions. From μ, U, and B, the value of h_o is calculated in Tables 1 and 2 for each design using Equation (7) as follows:

$$h_o = 0.264 \left[\left(\frac{\mu U}{PB} \right) (B^2) \right]^{1/2}$$

The load P is calculated from the value $\mu U/PB$ since it did not always correspond to a data point where the load was known. The maximum loads under hydrodynamic conditions for the centered bearings indicate that three bearing types did better than the tilt-pad bearing. They are the hybrid-pad with a 5.08 cm (2.00 in.) radius, the swing-pad with a 2.54 cm (1.00 in.) radius, and the swing-pad with a 10.16 cm (4.00 in.) radius. The load-carrying capacity was increased by 79, 54, and 27 percent, respectively, compared with the tilt-pad. When the pads were offset, however, the tilt-pad carried the most load.

In the case of the elastomeric swing-pad bearings, the best performance was obtained with the smallest radius of curvature. As the radius increased, load-carrying capacity decreased. The hybrid-pad did not show such a clear-cut trend. The 2.54 cm (2.00 in.) radius had the best overall performance. The 10.16 cm (4.00 in.) radius was worse in all cases, as expected. The 2.54 cm (1.00 in.) radius showed a surprisingly poor performance in all tests except for the centered position in the transition zone. Upon closer inspection of this bearing, it was

TABLE 1 - LAST HYDRODYNAMIC VALUES FOR CENTERED BEARINGS

Bearing Type	$\frac{\mu U}{PB}$	f, Coefficient of Friction	ho, Calculated μm (μin.)	P, Calculated kPa (psi)	Relative Ranking (Tilt-Pad=1.00)
Hybrid-Pad* R=2.00 in. Centered 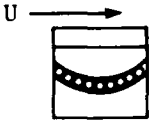	4.8×10^{-8}	0.00094	1.8 (72.0)	7,033 (1,020)	1.79
Swing-Pad R=1.00 in. Centered 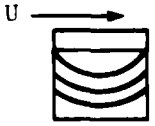	5.6×10^{-8}	0.00103	2.0 (78.1)	6,026 (874)	1.54
Swing-Pad* R=2.00 in. Centered 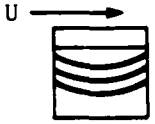	6.8×10^{-8}	0.00110	2.2 (86.0)	4,964 (720)	1.27
Tilt-Pad* Centered 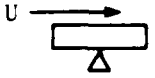	8.6×10^{-8}	0.00102	2.5 (97.0)	3.923 (569)	1.00
Hybrid-Pad R=1.00 in. Centered 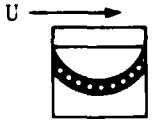	1.1×10^{-7}	0.00240	2.8 (109.0)	3,068 (445)	0.78
Hybrid-Pad R=4.00 in. Centered 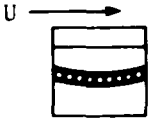	1.2×10^{-7}	0.00119	2.9 (114.0)	2,813 (408)	0.72
Swing-Pad R=4.00 in. Centered 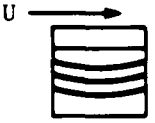	1.2×10^{-7}	0.00167	2.9 (114.0)	2,813 (408)	0.72
Swing-Pad R= ∞ Centered 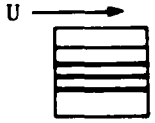	1.3×10^{-7}	0.00163	3.0 (119.0)	2,599 (377)	0.66

*Previously tested.[2]

TABLE 2 - LAST HYDRODYNAMIC VALUES FOR OFFSET BEARINGS

Bearing Type	$\frac{\mu U}{PB}$	f, Coefficient of Friction	ho, Calculated μm (μin.)	P, Calculated kPa (psi)	Relative Ranking (Tilt-Pad=1.00)
Tilt-Pad* U x/B=0.7 in.	4.3×10^{-8}	0.00078	1.8 (68.0)	7,853 (1,139)	1.00
Swing-Pad* U R=2.00 in. x/B=0.7	5.2×10^{-8}	0.00098	1.9 (75.0)	6,495 (942)	0.83
Swing-Pad U R=1.00 in. x/B=0.7	5.3×10^{-8}	0.00077	1.9 (76.0)	6,433 (933)	0.82
Hybrid-Pad* U R=2.00 in. x/B=0.7	5.5×10^{-8}	0.00088	1.9 (77.0)	6,136 (890)	0.78
Hybrid-Pad U R=4.00 in. x/B=0.7	5.6×10^{-8}	0.00101	2.0 (78.1)	6,026 (874)	0.77
Swing-Pad U R= ∞ x/B=0.7	6.2×10^{-8}	0.00096	2.1 (82.0)	5,447 (790)	0.69
Swing-Pad U R=4.00 in. x/B=0.7	6.4×10^{-8}	0.00092	2.1 (83.5)	5,275 (765)	0.67
Tilt-Pad U x/B=0.6	6.7×10^{-8}	0.00095	2.2 (85.4)	5,040 (731)	0.64
Hybrid-Pad U R=2.00 in. x/B=0.6	8.8×10^{-8}	0.00120	2.5 (97.9)	3,834 (556)	0.49
Hybrid-Pad U R=1.00 in. x/B=0.7	1.5×10^{-7}	0.00200	3.3 (128.0)	2,248 (326)	0.29

*Previously tested.[2]

TABLE 3 - LAST TRANSITION VALUES FOR CENTERED BEARINGS

Bearing Type	$\frac{\mu U}{PB}$	f, Coefficient of Friction	P, Calculated kPa (psi)	Relative Ranking (Tilt-Pad=1.00)
Hybrid-Pad R=1.00 in. Centered 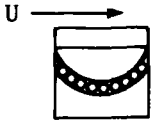	1.3×10^{-8}	0.00380	25,996 (3,766)	2.23
Hybrid-Pad* R=2.00 in. Centered 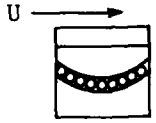	1.7×10^{-8}	0.00120	19,857 (2,880)	1.71
Swing-Pad R=1.00 in. Centered 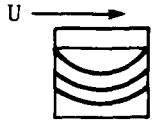	1.8×10^{-8}	0.00083	18,754 (2,720)	1.61
Swing-Pad* R=2.00 in. Centered 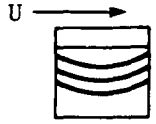	2.8×10^{-8}	0.00145	12,059 (1,749)	1.04
Tilt-Pad* Centered 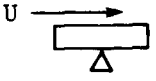	2.9×10^{-8}	0.00096	11,638 (1,688)	1.00
Swing-Pad R=∞ Centered 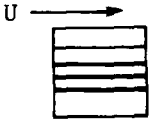	2.9×10^{-8}	0.00183	11,639 (1,688)	1.00
Swing-Pad R=4.00 in. Centered 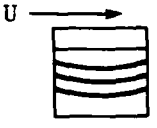	2.9×10^{-8}	0.00185	11,639 (1,688)	1.00
Hybrid-Pad R=4.00 in. Centered 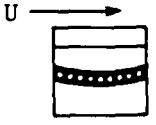	3.5×10^{-8}	0.00230	9,646 (1,399)	0.83

*Previously tested.[2]

TABLE 4 - LAST TRANSITION VALUES FOR OFFSET BEARINGS

Bearing Type	$\frac{\mu U}{PB}$	f, Coefficient of Friction	P, Calculated kPa (psi)	Relative Ranking (Tilt-Pad=1.00)
Swing-Pad R=1.00 in. x/B=0.7 	1.2×10^{-8}	0.00113	28,407 (4,120)	1.35
Swing-Pad* R=2.00 in. x/B=0.7 	1.2×10^{-8}	0.00093	28,131 (4,080)	1.33
Swing-Pad R=∞ x/B=0.7 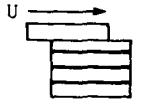	1.4×10^{-8}	0.00072	24,111 (3,497)	1.14
Tilt-Pad* x/B=0.7 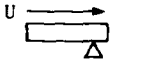	1.6×10^{-8}	0.00086	21,098 (3,060)	1.00
Hybrid-Pad* R=2.00 in. x/B=0.7 	1.6×10^{-8}	0.00090	21,098 (3,060)	1.00
Swing-Pad R=4.00 in. x/B=0.7 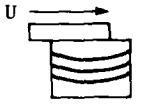	1.7×10^{-8}	0.00083	19,857 (2,880)	0.94
Hybrid-Pad R=4.00 in. x/B=0.7 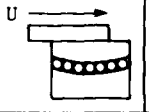	1.8×10^{-8}	0.00092	18,754 (2,720)	0.89
Tilt-Pad x/B=0.6 	2.1×10^{-8}	0.00105	16,072 (2,331)	0.76
Hybrid-Pad R=2.00 in. x/B=0.6 	4.9×10^{-8}	0.00128	6,888 (999)	0.33
Hybrid-Pad R=1.00 in. x/B=0.7 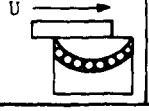	1.1×10^{-7}	0.00207	3,068 (445)	0.15

*Previously tested.[2]

observed that the assembly had a small amount of wobble. The radii of curvature in the mounting plate and in the support platform did not exactly conform with the ball path diameter. It is quite conceivable that the poorer-than-expected performance of this bearing can be attributed to the problem described.

Offsetting the pad surface to x/B = 0.7 improved performance for all the elastomeric swing-pad and the tilt-pad bearings. The hybrid-pad showed improvement only for the 10.16 cm (4.00 in.) radius when offset. Tests were conducted with offset of x/B = 0.6 for the tilt-pad and hybrid-pad bearings with a 5.04 cm (2.00 in.) radius. The results show that bearings with x/B = 0.7 performed better.

The constraints limiting the extension of hydrodynamic behavior appear to be the film thickness.[10,11,12,13] Calculated minimum film thicknesses from Tables 1 and 2 range from 1.8 to 3.3 μm (72.0 to 128.0 μin.). According to Reference 12, asperity contact initiates when the lubricant film thickness is about 10 times the order of the rms surface finish. The average surface roughness of the runner in the direction of motion is 0.15 μm to 6.0 μin.) rms. The expected limit is therefore 1.5 μm rms (60 μin.), which is close to values calculated from the experiments.

CONCLUSIONS

Based upon a single set of tests on each bearing design, the following conclusions are made.

1. Below bearing unit loads of 2,248 kPa (326 psi), all bearing designs exhibited behavior characteristic of hydrodynamic conditions.

2. The maximum load under hydrodynamic conditions for the centered designs showed an improvement of 79 percent for the hybrid-pad bearing and 54 and 27 percent for two swing-pad designs, respectively, over the tilt-pad bearings.

3. Decreasing the radius of curvature for the elastomeric swing-pad bearing in the range tested herein increases its load capacity.

4. Improvements in hydrodynamic performance of both the tilt-pad and laminated elastomeric swing-pad bearings were observed by offsetting the pad surfaces.

5. The best offset performance was at x/B = 0.7 for all bearings tested.

6. The transition region from hydrodynamic behavior to the point at which the coefficient of friction increases abruptly with increased load is extended in all designs by offsetting the pad surfaces.

REFERENCES

1. Greene, J., "The Swing-Pad Bearing - A New Concept in Sliding-Surface Bearings," DTNSRDC Report 76-0055 (Dec 1976).

2. Sides, T. and T. Daugherty, "Frictional Characteristics of Tilt-Pad and Swing-Pad Thrust Bearings," DTNSRDC Report 80/101 (Sep 1980).

3. Fuller, D., "Theory and Practice of Lubrication for Engineers," John John Wiley and Sons Inc, New York (1955).

4. Cameron, A., "Basic Lubrication Theory," 2nd ed., Ellis Horwood Ltd.(1976).

5. Raimondi, A.A. and J. Boyd, "Applying Bearing Theory to the Analysis and Design of Pad-Type Bearings," Transactions of Amer. Soc. Mech. Eng. (Apr 1955).

6. Pinkus, O. and B. Sternlicht, "Theory of Hydrodynamic Lubrication," McGraw-Hill, New York (1961).

7. Raimondi, A.A. and J. Boyd, "The Influence of Surface Profile on the Load Capacity of Thrust Bearings with Centrally Pivoted Pads," Transactions of the Amer. Soc. Mech. Eng. (Apr 1955).

8. Hersey, M.D., "Theory and Research in Lubrication," J. Wiley and Sons, New York (1966).

9. O'Connor, J.J. and J. Boyd, "Standard Handbook of Lubrication Engineering," Editors, McGraw-Hill Co., pp. 5-23 (1968) ff

10. Kreisle, L.F., "Predominant-Peak Surface Roughness, a Criterion for Minimum Hydrodynamic Oil-Film Thickness of Short Journal Bearings," Transactions of the Amer. Soc. Mech. Eng. (Aug 1957).

11. Ledocq, H.M., "The Transition from Hydrodynamic to Boundary Regime of Tilting-Thrust Pads," Tribology (Feb 1974).

12. Elwell, R.C. and E.R. Booser, "Low Speed Limit of Lubrication," Machine Design (15 Jun 1972).

13. Gardner, W.S., "Journal Bearing Operation at Low Sommerfeld Numbers," Amer. Soc. Lub. Eng. Transactions, Vol. 19, No. 3, pp. 187-194 (May 1975).

INITIAL DISTRIBUTION

Copies

9 NAVSEA
- 1 SEA 05
- 3 SEA 05DC
- 1 SEA 05R
- 1 SEA 052
- 1 SEA 524
- 2 SEA 99612

12 DTIC

CENTER DISTRIBUTION

Copies	Code	
1	012	Dr. Allen
1	1102	R.M. Stevens
1	272	Dr. Quandt
1	2723	Mr. Strucko
1	2802	Dr. Kramer
1	283	Dr. Bosmajian
12	2832	N.T. Sides
12	2832	T.L. Daugherty
10	5211.1	Rept Distribution
1	522.1	Class Lib (C)
1	522.2	Class Lib (A)
2	5231	Office Services (A)

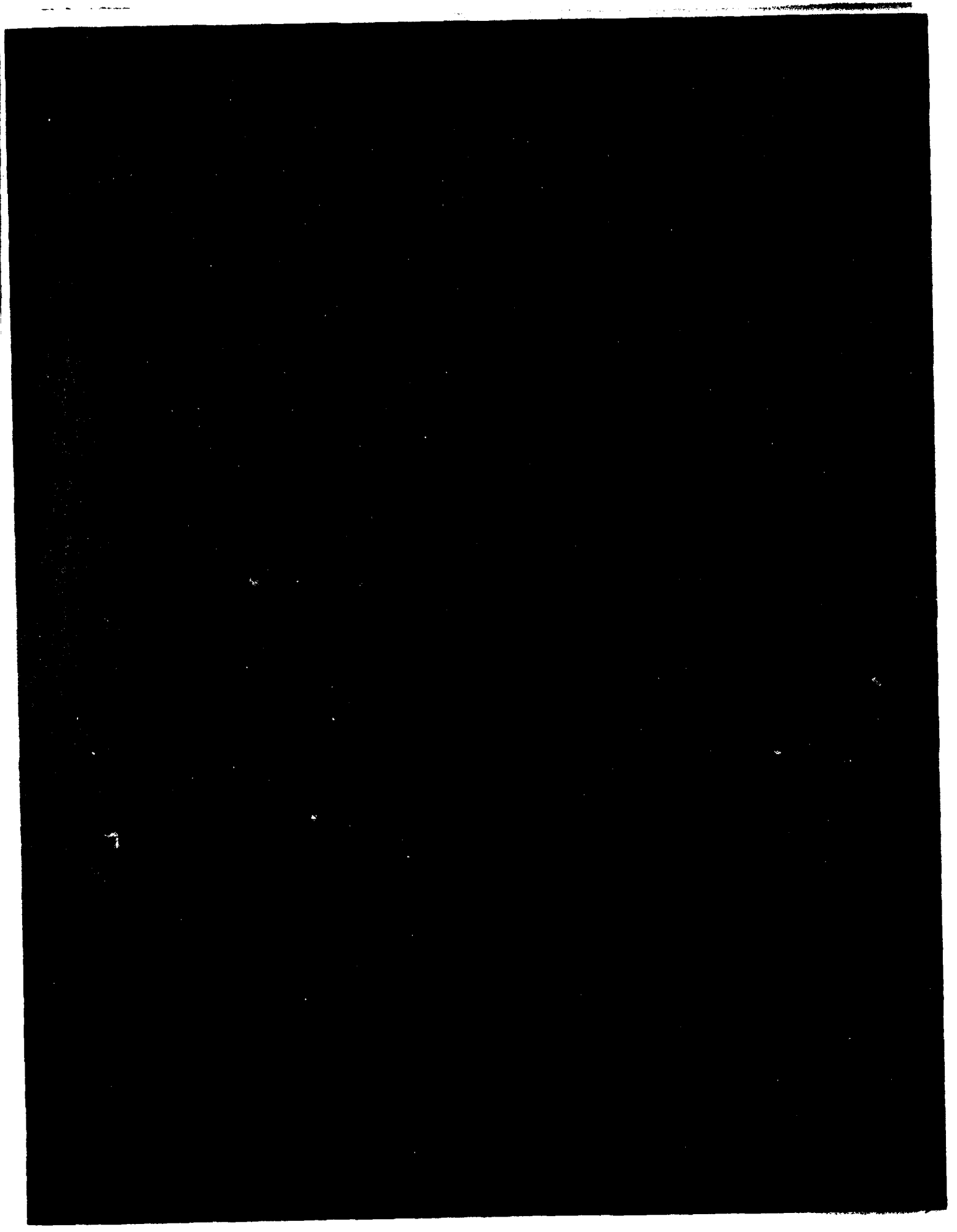

END

DATE
FILMED

8

DTIC